Journal of Materials and Environmental Sciences
ISSN : 2028-2508

J. Mater. Environ. Sci., 2017 Volume 8, Issue 11, Page 4125-4137

http://www.jmaterenvironsci.com/

Preparation and characterization of activated carbons from olive wastes by physical and chemical activation: Application to Indigo carmine adsorption

G. Enaime[1], K. Ennaciri[1], A. Ounas[1], A. Baçaoui[1], M. Seffen[2], T. Selmi[2], A. Yaacoubi[1*]

[1]*Laboratory of Applied Chemistry (LCA), Faculty of Sciences Semlalia, Cadi Ayyad University, B.P 2390 Marrakech, Morocco.*

[2]*Laboratory of Energy and Materials (LABEM). High School of Sciences and Technology of Hammam Sousse, BP 4011, Hammam Sousse, Sousse University, Tunisia.*

Received 29 Jul 2016,
Revised 09 Nov 2016,
Accepted 13 Nov 2016

Keywords

- ✓ Indigo carmine dye;
- ✓ Activated carbon;
- ✓ Adsorption isotherm;
- ✓ Kinetics;
- ✓ Thermodynamics

A. Yaacoubi
ayaacoubi@uca.ac.ma
Phone: +212661885342

Abstract

Present study explored the adsorptive characteristics of Indigo Carmine (IC) dye from aqueous solutions onto activated carbon (AC) prepared from olive solid waste (OSW) impregnated with olive mill wastewater (OMWW) by chemical activation using potassium hydroxide (KOH) and phosphoric acid (H_3PO_4) as activation agents and physical activation using steam. The adsorbents were characterized by BET surface area, FTIR spectra, scanning electron microscopy (SEM), iodine number and methylene blue adsorption. Influence of contact time, initial concentration (10–250 mg/L) and temperature (293–323 K) on adsorption capacity was investigated. The results shows that at all temperatures and for all initial concentrations the carbon activated by KOH agent exhibit the best adsorption capacity followed by steam activated carbon and at last the carbon activated by H_3PO_4. Adsorption data were modeled using the pseudo-first-order, pseudo-second-order and intra-particle diffusion kinetic equations. It was shown that pseudo-second-order kinetic equation could best describe the adsorption kinetics. The equilibrium adsorption data of IC dye on activated carbon samples were analyzed by Langmuir and Freundlich models. The results indicate that the Freundlich model provides the best correlation of the experimental data. Adsorption of IC on activated carbon samples was favorably influenced by temperature. The positive values of the enthalpy change indicate that adsorption is endothermic. The results of this work indicate that activated carbon prepared from olive waste (OW) is suitable as adsorbent material for adsorption of IC dye from aqueous solutions.

1. Introduction

Several industries, such as textile, clothing, refineries, dyestuff, leather, rubber, plastic, paper and food processing, discharge wastewaters in aqueous environments. Because of their persistent color, low biodegradability, high pH and temperature [1] these effluents can be considered as potential sources of pollution.

Among the most useful dyes, there is indigo carmine. It is widely used in textile, food and cosmetics industries. The carmine indigo is known by its toxicity, contact with it can cause skin and eye irritations and also permanent injury to cornea and conjunctiva to human being. The consumption of the dye can lead to reproductive, neuro and acute toxicity [2]. Indigo carmine causes irritation to the respiratory tract such as coughing and shortness of breath [3].

Various technologies have been studied in order to separate Indigo Carmine from water and wastewater such as electrochemical [4, 5], photochemical [6], photocatalytic treatment [7] and biological methods [8]. Out of all the aforementioned techniques, adsorption has become a well-know alternative process for the removal of soluble pollutants from aqueous solution. Several adsorbents have been used to adsorb Indigo carmine dye from aqueous solutions, including nut shells [9], chitin and chitosan [10], Fe-zeolitic tuff [2] and Rice husk ash [3]. Activated carbon has been one of the most used adsorbent to remove soluble compounds from water because of its large surface area, well developed porosity, and high adsorption capacity [11]. Nevertheless, the use of commercial activated carbon is limited because of its high cost suggesting to use low-cost agricultural wastes, such as hardwood [12], spent coffee [13], lignin [14], coconut husk [15], pomegranate leaves [16] and olive waste [17] as a precursors for preparation of activated carbon that can be used as alternative adsorbents for the wastewater treatment.

The valorization of olive wastes, as a carbonaceous biomass generated intensively in Morocco, to produce activated carbon with high quality can be a promising and economical alternative. For this purpose, a mixture of olive solid waste and olive mill wastewater has been used as precursor to prepare activated carbon by chemical activation using KOH and H_3PO_4 as activation agents and by physical activation using steam. The prepared activated carbons were characterized and tested for its ability to remove IC from aqueous solutions. The effect of different parameters such as contact time, initial IC concentration and temperature were investigated. Finally, the kinetic and isotherm as well as the thermodynamic parameters for the adsorption of IC dye onto the activated carbons were evaluated.

2. Materials and methods

2.1. Adsorbate

Indigo carmine (IC) dye or Acid Blue 74 is a dark blue, water-soluble powder having molecular formula $C_{16}H_8N_2Na_2O_8S_2$ with two sulfonate groups. The general characteristics of this dye are: molar mass = 466.35 g/mol, color index number = 73015, and maximum light absorption at 608 nm.

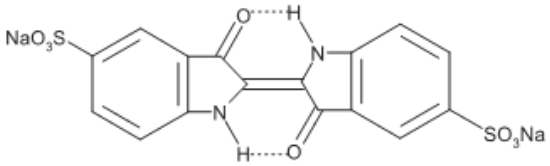

Figure 1: Chemical structure of indigo carmine (IC).

2.2. Activated carbon

In the present study, a mixture of OSW and OMWW collected from a three-phase mill located in the area of Marrakech (Morocco) were used as raw material to produce activated carbon via chemical activation using KOH and H_3PO_4; and physical activation using steam. Experiments were carried out in a reactor inserted into a tubular regulated furnace.

The preparation of the mixture of OSW and OMWW was conducted as follows: A mass of 1kg of waste water was added to 500 g of OSW, and stirred in order to promote the homogenization of the mixture, which was then dried at room temperature and weighed regularly to constant mass.

25 g of dried precursor (OMWW+OSW) was mixed with H_3PO_4 or KOH solutions and then heated at 383 K to total evaporation. The impregnation ratio, defined by the weight ratio of impregnant (KOH or H_3PO_4) to precursor, was 2 for KOH and 4 for H_3PO_4. For sample activated with KOH, the impregnated precursor was introduced into the reactor which was then heated to the desired temperature (573 K) and maintained for 3 h at the final temperature under nitrogen flow. After carbonization we proceed to activation at 1073 K during an activation time of 1h. For H_3PO_4 the activation was carried out in one step, 25 g of the impregnated material was conducted in the reactor. The temperature and time of activation were maintained at 1073 K and 1 h, respectively, and the system was kept under continuous nitrogen flow. After cooling down to room temperature, the obtained activated carbons was thoroughly washed with hot distilled water until it reached neutral, dried and crushed.

For physical method, carbonization and activation were carried out in one step [18]. A known amount of olive stones (25 g) was introduced into the reactor which was heated to the desired temperature under nitrogen flow. For activation process, a steam generator was placed at the entrance of the reactor. The time and temperature of activation were, respectively, 1 h and 1123 K. After activation, the activated carbon were washed in distilled water, dried and crushed. The nomenclature and operation conditions of different samples, prepared by the method of chemical activation with KOH and H_3PO_4 and physical activation with steam, are summarized in Table 1.

Table 1: Preparation conditions of activated carbon samples from olive waste with chemical and physical activation.

Materials	Conditions of preparation						
	Carbonization				Activation		
	T (K)	Time (h)	N_2 (mL/min)		T (K)	Time (h)	Impregnation
KOH-activated OW (KOH-AC)	573	3	300		1073	1	KOH
H_3PO_4-activated OW (H_3PO_4-AC)	-	-	-		1073	1	H_3PO_4
Steam-activated OW (Steam-AC)	-	-	-		1123	1	-

2.3. Characterization

N_2 adsorption at 77 K was used to determine specific surface areas, pore volume and pore size distribution of carbon samples. The surface area (S_{BET}) of the sorbents was calculated by applying the BET (Brunauer–Emmet and Teller) model of isotherms. Total pore volume (V_T) was determined from the amount of N_2 adsorbed at p/p_0 = 0.95. Micropore surface area (S_{mic}) and micropore volume (V_{mic}) was determined by Dubinin-Radushkevich equation (DR) applied to N_2 adsorption data. The mesopore surface area (S_{mes}) and mesopore volume (V_{mes}) were calculated by subtracting the micropore surface area from total surface area and the micropore volume from total pore volume, respectively.

The FTIR spectra and scanning electronic microscopy SEM are of great help to get information about functional groups and morphology of activated carbon samples, respectively.

The iodine number can be used as an index to get a good simulation of surface area and internal structure of carbons. Generally high adsorption capacity of iodine corresponds to high surface area and well developed micoporosity of adsorbent [19]. The iodine adsorption was determined using the sodium thiosulfate volumetric method [20].

The adsorption of methylene blue ($C_{16}H_{18}N_3SCl$), the most recognized molecule to evaluate the adsorption capacity of adsorbents to adsorb molecules into meso and macropores, onto the activated carbon samples was carried out by adding 0.01 g of each carbon to flasks containing 100 mL of methylene blue solution with initial concentration of 300 mg/L. The suspensions were stirred at room temperature until reaching the equilibrium time (4h determined by kinetic tests) and filtered using a 0.45 µm filter. The residual concentration values were measured by spectrophotometric method at the characteristic wavelength 660 nm corresponding to the maximum absorbance.

2.4. IC adsorption experiments

Batch experiments were conducted to study the adsorption kinetics, adsorption isotherms and the effect of temperature on IC adsorption onto activated carbon samples.

According to some previous studies [21, 22]examining the adsorptive removal of IC onto different adsorbents and some preliminary tests performed in the present study, a pH of 2 was chosen as selective pH for subsequent experiments. The pH was adjusted by adding dilute aqueous solutions of HCl or NaOH (1M).

In order to study the adsorption kinetics, a 100 mL of dye solution with concentration of 20 mg/L and a known adsorbent dose were taken in Erlenmeyer flasks. This mixture was agitated in a temperature controlled batch at a constant speed of 150 rpm. To ensure good dispersion of solid particles of activated carbon and good adsorption kinetics, we adopted the value of 0.1 g /L (or 10 mg/100 mL) for solid / liquid ratio. The adsorption kinetics was determined by analyzing adsorptive uptake of dye solution at different reaction times.

Regarding the adsorption isotherms, IC solutions with different concentrations, varied from 20 to 250 mg/L, was agitated with 10 mg of adsorbent over night to be sure that the equilibrium will be achieved. The effect of temperature on the sorption characteristics was investigated by determining the adsorption capacities at 293, 308 and 323 K for solution initial concentration of 20 mg/L. Blank experimental runs, with only the adsorbent in distilled water, were conducted simultaneously at similar conditions to account for experimental conditions.

The spectral evolution and the measurements of the optical density of IC solutions at different reaction times were carried out using UV/vis spectrophotometer at the characteristic wavelength corresponding to maximum absorbance (608 nm). The values of the residual concentrations were obtained by interpolation using the calibration curve between absorbance and the concentration of the dye solution. Adsorptive removal of IC was calculated, from measured residual concentrations, by the formula:

$$q_a = \frac{(C_i - C_f) \times V}{m} \qquad (1)$$

Where, q_a (mg/g), C_i (mg/L) and C_f(mg/L) are the amount of adsorbed IC, the initial and the final concentration of IC in the solution, respectively. V (mL) is the volume of dye solution and m (mg) is the masse of adsorbent.

3. Results and discussion

3.1. Characterization

3.1.1. Surface areas, BET (S_{BET})

The N_2 adsorption–desorption isotherms at 77 K for the prepared activated carbons are shown in Figure 2, and the textural characteristics obtained from the isotherms are summarized in Table 2 (BET surface area; S_{BET}, micropore surface area; S_{mic}, mesopore surface area; S_{mes}, micropore volume; V_{mic}, mesopore volume; V_{mes}). As shown in Figure 2 the KOH-AC and Steam-AC isotherms exhibit a sharp increase in the adsorbed volume at low relative pressures ($P/P_0 < 0.01$). This type of isotherm belongs to the type I of the IUPAC classification,

characteristic of microporous material with small pore sizes and also indicative of the monolayer adsorption [23]. Furthermore, Steam-AC desorption isotherm present closure at P/P_0~0.4, which is characteristic of type-IV isotherm implying that this activated carbon exhibits both micro and mesoporous structure.

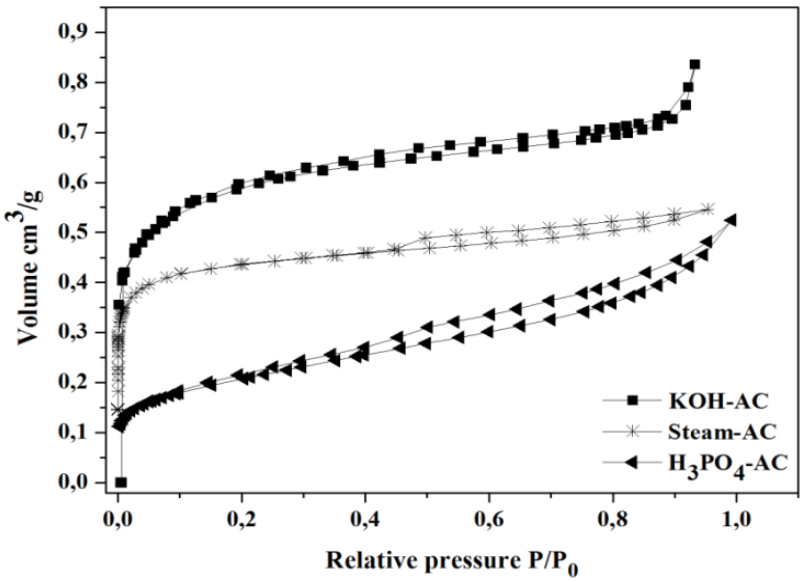

Figure 2: N_2 (77 K) adsorption–desorption isotherms of activated carbons.

Similar to KOH-AC and Steam-AC, the H_3PO_4-AC presented an increase in the adsorption volume up to a p/p_0~0.1 attributed to the presence of micropores. However, the adsorbed volume keeps increasing for the whole range of p/p_0 which could be explained by the mesoporous structure of H_3PO_4-AC sample.
We observed also, for KOH-AC and H_3PO_4-AC, at a high relative above 0.9, a steep increase in the slope indicates capillary condensation in mesopores [23].
The BET measurements, Table 2, show that the sample of olive waste impregnated with KOH followed by sample physically activated has the highest specific surface area (1375 and 1065 m^2/g respectively) compared to the sample impregnated with H_3PO_4 (466 m^2/g). Furthermore, the ratios between micropores surface area and the total specific surface area, S_{micro}/S_{BET}, are 0.62 for KOH-AC, 0.75 for Steam-AC and 0.54 for H_3PO_4-AC.
As the result shows, the sample activated with KOH exhibit a higher surface area and a developed micropore structure which could be attributed to the following mechanism [24]: the KOH is dehydrated to produce K_2O, the reaction of K_2O with CO_2, resulted from the water-shift reaction, give K_2CO_3. The formation of metallic potassium at a temperature above 700 °C could cause a drastic expansion of the carbon structure and create a large specific surface area and a high pore volume. However, the carbon prepared by steam activation method has much larger micro-pore surface than KOH-AC, this is consistent with the fact that water vapor has the ability to penetrate into solid structure and facilitate desorption and removal of volatiles from materials [25] results in development micropores, while activation with H_3PO_4 promotes the decomposition of the initial organic material and the formation of cross-linked structure in the precursor leading to produces the pore size distribution located in the mesopore range [26]. The mircropore volume ratios, V_{micro}/V_t, are 0.64 for KOH-AC, 0.74 for steam-AC and 0.40 for H_3PO_4-AC, supporting the last found that activation with KOH and steam allow producing carbons with micropore texture.

Table 2: Textural characteristics and experimental results of adsorption test of characteristic molecules of activated carbon samples from olive waste with chemical and physical activation.

Materials	Textural characteristics						Adsorption test of characteristic molecules	
	BET (m^2/g)	S_{mic} (m^2/g)	$S_{més}$(m^2/g)	$V_{0.95}$ (cm^3/g)	V_{mic} (m^3/g)	V_{mes} (cm^3/g)	Iodine number (mg/g)	MB adsorption (mg/g)
KOH-AC	1375	853	522	0.84	0.52	0.30	1136	536
H_3PO_4-AC	466	250	216	0.46	0.18	0.27	435	331
Steam-AC	1065	798	267	0.55	0.41	0.14	1153	500
Commercial AC	864	-	-	-	-	-	1049	240

3.1.2. FTIR spectra

The FTIR spectra of the activated carbon samples were given in Figure 3. For KOH-AC, the band in the range of 3774 cm^{-1} was associated with hydrogen bonds, which were formed between water and protons of acidic groups, the band observed at 3452 cm^{-1} is assigned to -OH vibration stretching of hydroxyl groups involved in hydrogen bonding possibly due to adsorbed water [27].The band centered at 2387 cm^{-1} is ascribed to C=C bond. The band located at 1595 cm^{-1} is due to stretching vibrations in aromatic rings, while the band in the range of 1068 cm^{-1} is attributed to the alcohol groups (R–OH).

The Steam-AC shows also a band at 3454 cm^{-1} corresponding to hydroxyl groups, a band at 1600 cm^{-1} stretching vibrations in aromatic rings. As observed for KOH-AC the band centered at 1072 cm^{-1} is assigned to the alcohol groups (R–OH). Concerning the sample corresponding to H_3PO_4-AC, the bands observed are: 3454 cm^{-1} corresponds to –OH vibration, 2389 cm^{-1} assigned to C=C bond, 1600 cm^{-1} assigned to the C-O stretching in aromatic rings. The bands observed at 1230 cm^{-1} and 1120 cm^{-1} could be assigned to the phosphorous species i.e. hydrogen-bonded P=O, O-C stretching vibrations in P-O-C of aromatics [28] and P=OOH [29], which suggests the incorporation of this element in the activated carbon structure.

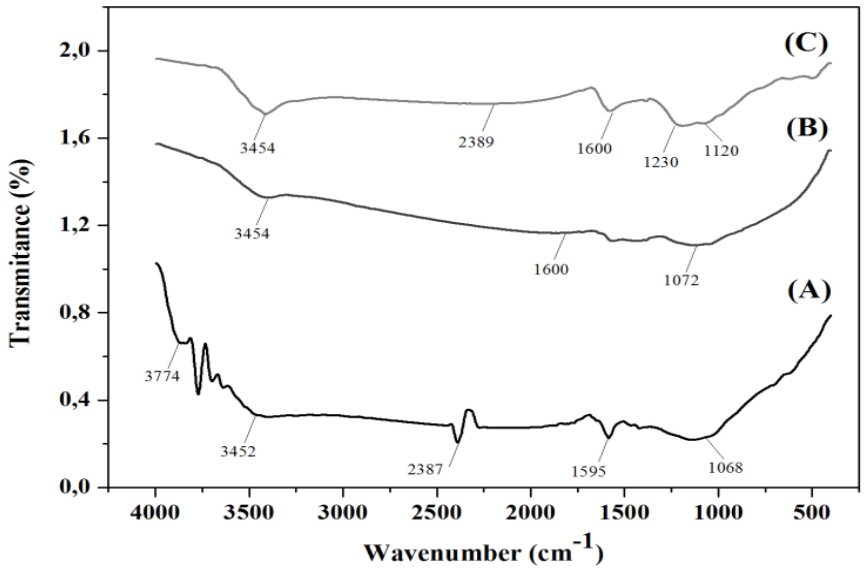

Figure 3: FTIR spectra of KOH-AC (A), Steam-AC (B) and H_3PO_4-AC (C) samples.

3.1.3. SEM micrographs

Scanning electron microscopy (SEM) was used to characterize the morphology and physical properties of prepared carbons. The SEM micrograph of KOH-AC (A), Steam-AC (B) and H_3PO_4-AC (C) samples are shown in Figure 4. It is clear that, samples appear to have important amount of pore allowing dye to be absorbed into these carbons.

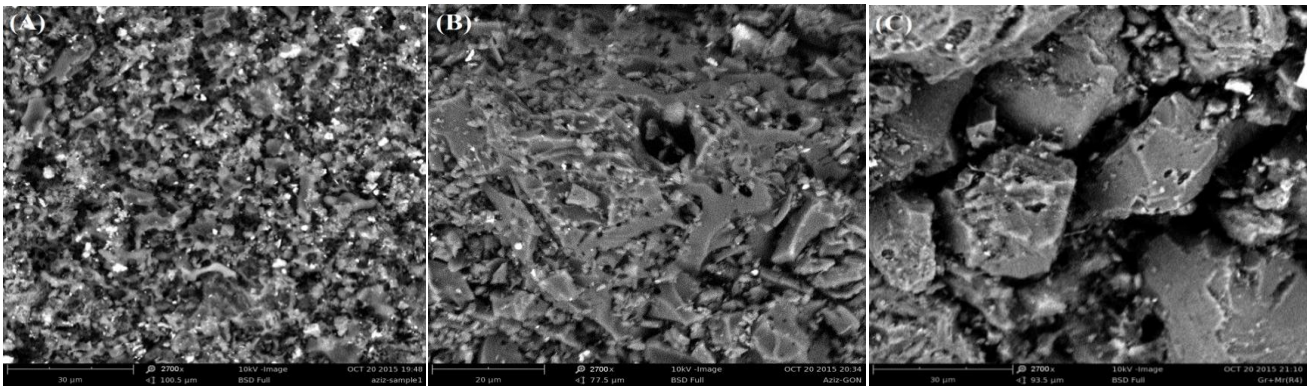

Figure 4: SEM images of KOH-AC (A), Steam-AC (B) and H_3PO_4-AC (C).

The comparison of the morphology of the three carbons, reveals that the activation with KOH allow to produce carbons with high developed micro and mesoporosity and homogeneous distribution of pores into surface of material, we can note that this carbon presented a large amount of pore situated in the narrow micropore range,

steam-AC exhibit a structure with both micro and mesopores, whereas H_3PO_4 activation developed carbon with a structure globally rich of pores with large size situated in the mesoporous range.

3.1.4. The iodine number and methylene blue adsorption

The data obtained for iodine adsorption (Table 2) indicate that KOH-AC and Steam-AC adsorb significant amounts of iodine compared to H_3PO_4-AC. In many activated carbons, there is a correlation between the adsorption of iodine and the BET surface areas [30]. However, adsorbents with much larger surface areas may have significant amount of narrow micropores causing lower ability of iodine to penetrate into pores and as consequence lower iodine numbers. The value of BET surface areas compared with iodine numbers of samples, suggest that KOH activation promote development of narrower micropores in carbon structures, which explains their relatively low adsorption (800 mg/g) compared with steam-activated carbon prepared at 1123 K, having a higher adsorption capacity of iodine (1153 mg/g) due to its high-developed porosity and its large amount of micropores. Phosphoric acid activated carbon, H_3PO_4-AC, adsorbs lower amounts of iodine (435 mg/g). This can be attributed to the low amount of micropores despite higher mesoporous content of this carbon, and probably is due to the highly acidic surface contaminated with abundant phosphate [31].

MB adsorption values for all samples are given in Table 2. As shown, the prepared activated carbons exhibit higher adsorption uptake of MB, it is depending essentially on the textural characteristics of adsorbent. Thus, for KOH-AC sample who presented a developed porous structure characterized by a higher micro and mesoporous volume and a larger specific surface area, the adsorption capacity is much important than the other two samplesHowever, there is a difference between Steam-AC and H_3PO_4-AC in term of MB uptake (500 and 331 mg/g, respectively); even they have a similar amount of mesopores. This indicates MB molecules are mainly adsorbed in the micropores in agreement with the result found by Benadjemia et al. [32].

3.2. IC adsorption experiments

3.2.1. Sorption kinetics

The adsorption kinetics of IC dyes was studied in order to investigate the mechanism of adsorption as a function of contact time and to determine the required time to get equilibrium. Figure 5 shows that, under the same conditions, indigo carmine does not have the same affinity in the face of various activated carbon samples.

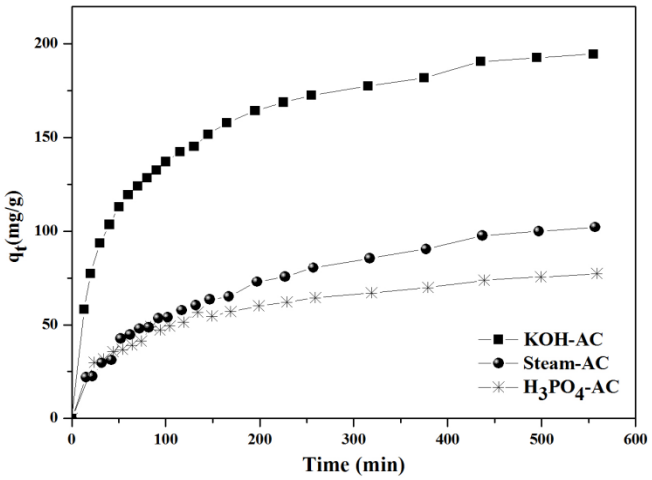

Figure 5: Adsorption kinetic of indigo carmine on activated carbon samples (adsorbent mass, 0.01 g; dye concentration, 20 mg/l).

It was observed as well that the adsorption rate was slightly higher for KOH-AC followed by Steam-AC and finally H_3PO_4-AC. Therefore, the adsorption capacity of IC on the activated carbon samples at equilibrium varies in the same order. This finding is strongly linked to the preparation method and structural properties of activated carbon samples. Thus, for KOH-AC sample who presented a developed porous structure characterized by a higher micro and mesoporous volume and a larger specific surface area, the adsorption capacity is much important than the other two samples. However, for Steam-AC and H_3PO_4-AC, they presented almost a similar behavior against IC with a slight difference in the adsorption capacity in favor of Steam-AC sample. Comparing the textural characteristics of these carbons, summarized in Table 2, it is noted that the surface area and volume of micropores are greater for carbon activated with steam as that activated with H_3PO_4, while the surface and volume of mesopores are similar for both adsorbents. Then the adsorption of IC onto prepared activated carbons is more important when the adsorbent presented a large amount of mesopores.

According to the Figure 5, the adsorption occurs in two stages: an initial fast and a second slower, we can note that over 95% of the adsorption capacity of each sample is reached in the first part. Beyond this time, the adsorption rate becomes progressively slower and the equilibrium was reached after a contact time depending on each sample (e.g.435 min, 437 min and 379 min for KOH-AC, H_3PO_4-AC and Steam-AC, respectively). This behavior is probably due to rapid and slow diffusion into meso and micropores of adsorbents, suggesting that adsorption process is probably controlled by boundary layer diffusion and intraparticle diffusion [9].
In order to investigate the mechanism of IC dye adsorption on activated carbon samples, several kinetic models were applied to the experimental data. The pseudo-first-order, pseudo-second-order and intra-particle diffusion models were employed to define the adsorption mechanism.
The model pseudo-first order was often expressed by Lagergren equation [33]. This model assumes that the sorption rate varies proportionally with solute concentration. The equation of model pseudo-first order is not applicable for the entire reaction time and is generally limited in the initial stage of adsorption process [34]:

$$\log(q_e - q_t) = \log q_e - \frac{k_1}{2{,}303}t \qquad (2)$$

With q_e the adsorption capacity at equilibrium (mg/L), q_t the adsorption capacity at time t (mg/L) and k_1 is the pseudo-first-order rate constant for the adsorption process (min^{-1}).
The slope of the linear fit of log (q_e-q_t) versus t (Figure 6) allows determining the value of k_1/2.303. The intercept of the straight line gives the value of log(q_e).

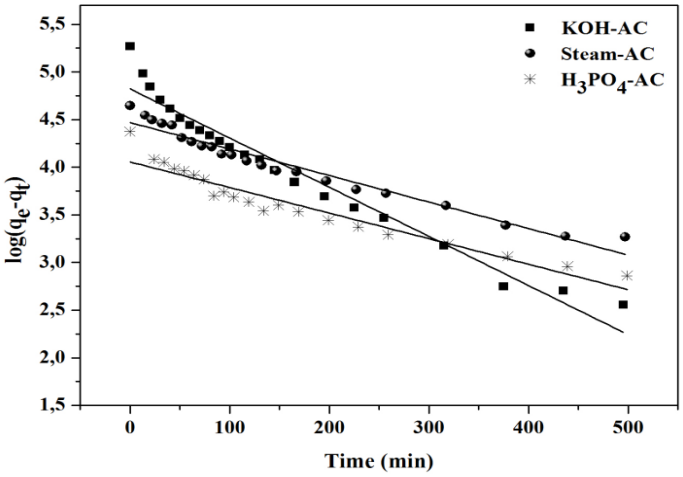

Figure 6: Pseudo-first-order kinetics of IC adsorption onto activated carbon samples.

The pseudo-second-order model suggests the existence of chemisorption [35]. It is represented by the differential equation as follow:

$$\frac{dq_t}{dt} = k^2(q_{eq} - q_t)^2 \qquad (3)$$

Where q_e is the amount of dye adsorbed at equilibrium (mg/g), q_t the amount of dye adsorbed at time t (mg/g), and k_2 is the equilibrium rate constant of pseudo-second-order sorption (g/mg min). Integrating Eq. (3) for the boundary conditions t=0 to t=t and q_t =0 to q_t =q_t gives:

$$\frac{t}{q_t} = \frac{1}{k_2 q^2_{eq}} + \frac{1}{q^2_{eq}}t \qquad (4)$$

The rate parameters k_2 and $q_e$can be directly obtained from the intercept and slope of the plot of t/q_t versus t (Figure 7).
Generally, a process is controlled by intraparticle diffusion, if its rate is proportionally related to the diffusion rate of each particle to another particle [36].
The intraparticle diffusion model proposed by Weber and Morris [37], was expressed by Eq.(5):

$$q_t = k_i t^{\frac{1}{2}} + C \qquad (5)$$

Where $q_t$is the amount of dye adsorbed at time *t* (mg/g), *t* the time (min), k_i the intraparticle diffusion rate constant (mg/g $min^{1/2}$) corresponding to the slopes of $q_t$versus $t^{1/2}$ plots (Figure 8), and *C* is the intercept (mg/g).
If intra-particle diffusion is rate-limited, the plots of square root of time $t^{1/2}$ versus adsorbate uptake $q_t$gives a straight line, and if this line passed through the origin, then the intraparticle diffusion is the only controlling step [34]. However, if the data present multi-linear plots, the sorption process can be influenced by two or more steps.

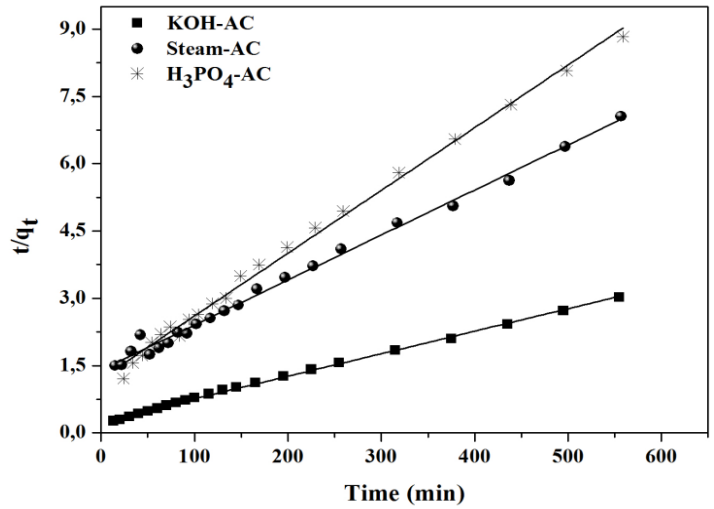

Figure 7: Pseudo-second-order kinetics of IC adsorption onto activated carbon samples.

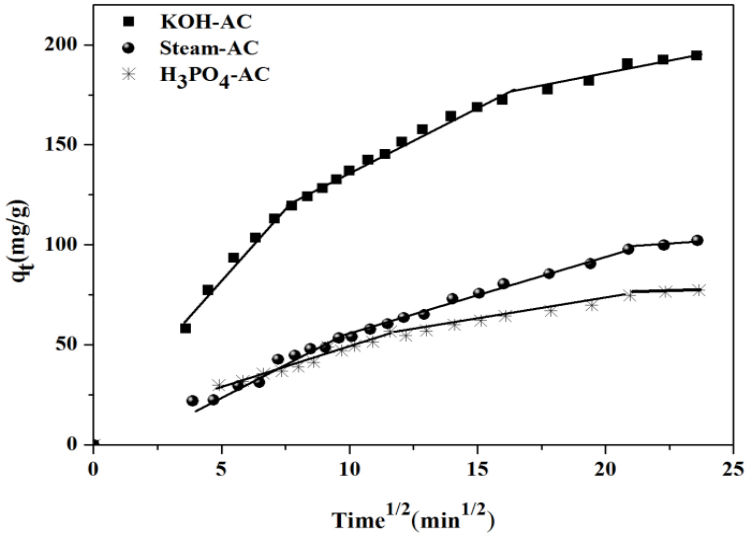

Figure 8: Amount of dye adsorbed vs.$t^{½}$ for intraparticle transport of IC by activated carbon samples.

The parameters obtained for the pseudo-first order, the pseudo-second order and the intra-particle diffusion models are presented in Table 3.

Table 3: Comparison of the pseudo-first-order, pseudo-second-order and intra-particle diffusion models for different samples of activated carbon.

Materials	q_{exp}	Pseudo-first order			Pseudo-second order			Intraparticle diffusion		
		q_{th} (mg/g)	k (min^{-1})	R^2	q_{th} (mg/g)	k (g/mg h)	R^2	C (mg/g)	k_i(mg/g $min^{1/2}$)	R^2
KOH-AC	194.54	124.27	0.0119	0.96	198.41	0.00010	0.99	53.44	7.49	0.90
H_3PO_4-AC	79.30	57.75	0.0062	0.92	70.47	0.00017	0.99	16.12	2.49	0.93
Steam-AC	104.17	87.34	0.0064	0.96	100.30	0.00007	0.99	7.69	4.35	0.97

Regarding the first-order model, the R^2 values shown in the Table 3 are significantly high. However, for all sorbents, the theoretical values of adsorbate uptake q_{th} calculated by this model are too low compared with experimental q_{exp} values. This finding suggested that the sorption process is not likely to obey a pseudo-first-order kinetic model. In addition, it was observed from the model curve, that the sorption data follow the Lagergren model only in the region where rapid sorption took place (for the initial sorption period), where plots of log (q_e−q_t) versus time showed a certain linearity, and thereafter the model is not applicable for the rest of reaction.

Unlike the first-order model, the plots of t/q_t versus t presented a straight line as showed in Figure 7, supporting that the sorption of IC onto carbons follow the pseudo-second-order. Thus for the pseudo-second-order kinetic

and for all samples, there is a good correlation between the q_{th} values calculated by this model and the experimental data, with higher values of R^2 (Table 3). The adsorption system was best described by the pseudo-second-order kinetic model for the entire sorption period which may indicate that the sorption process is rapid and may be chemical sorption probably taking place via surface exchange reactions until the molecules occupied all surface functional sites. [34]

Regarding the diffusion model, the R^2 values founded are between 0.90 and 0.97 (Table 3), indicates that the adsorption of IC can be controlled by an intraparticle diffusion model. Figure 8 presents the amount of dye adsorbed versus $t^{1/2}$ for all adsorbents. The plots presented multilinearity, which indicate two or more steps influenced the sorption. Thus for all samples, there are three linear portions, the first straight portion depicting boundary layer diffusion or mesopore diffusion, the second representing micropore diffusion while the third part corresponding to the final equilibrium stage where the sorption rate starts to slow down. According to the results shown in Table 3, for all samples the plots do not pass through the origin (the intercepts have a values in the range of 0.76–41.13 mg/g), suggesting that sorption process follows the intraparticle diffusion but it is not the only controlling mechanism.

3.2.2. Adsorption isotherms

The adsorption isotherms were performed using different initial concentrations between 20 and 250 mg/L, with a solid / liquid ratio of 0.01 g/100 mL. The adsorption isotherms of the three samples (Figure 9) indicate that as the initial dye concentration increases, the adsorption capacity increases, this reflects reduced free sites as the progression of the adsorption. Because of their simplicity, Langmuir and Freundlich isotherms, two widely used models, will be applied to analyze the experimental data.

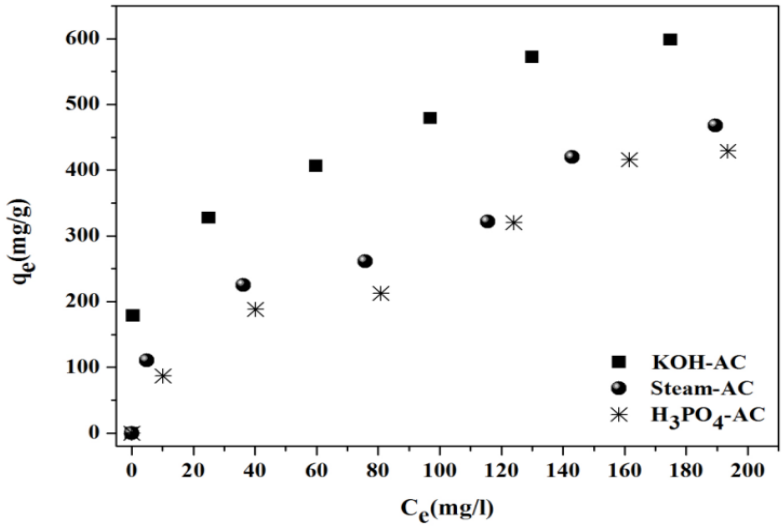

Figure 9: Adsorption isotherms for IC dye on activated carbon samples, adsorption time = 720 min.

The Langmuir isotherm is the most popular isotherm model. It suggested that maximum sorption corresponds to a monolayer adsorption of dye molecules on solid surface possessing a finite number of sorption sites [38].

The Langmuir model is represented by Eq.6 [39]:

$$q_e = \frac{q_{max}\, k_L C_e}{1+k_L C_e} \qquad (6)$$

Eq. (6) can be rearranged to a linear form:

$$\frac{C_e}{q_e} = \frac{1}{k_L . q_m} + \frac{C_e}{q_m} \qquad (7)$$

The value of k_L is related to the strength of interaction between the adsorbed molecules and the solid surface; q_m value expresses the amount of dye molecules adsorbed per gram of solid, forming monolayer on the homogenous surface of adsorbent.

The Freundlich equation is an empirical equation applies to adsorbents with heterogeneous surfaces [40], which is characterized by the heterogeneity factor $1/n_F$. The Freundlich isotherm equation can be written as follow [41]:

$$q_e = k_F C_e^{\frac{1}{n_F}} \qquad (8)$$

The linear form of this equation is given by:

$$\mathrm{Ln}\, q_e = \mathrm{Ln} k_F + \frac{1}{n_F} \mathrm{Ln} C_e \qquad (9)$$

Where q_e is the adsorption capacity at equilibrium (mg/g), C_e the equilibrium concentration in the liquid phase (mg/L), k_F the Freundlich constant and $1/n_F$ is the factor of heterogeneity.

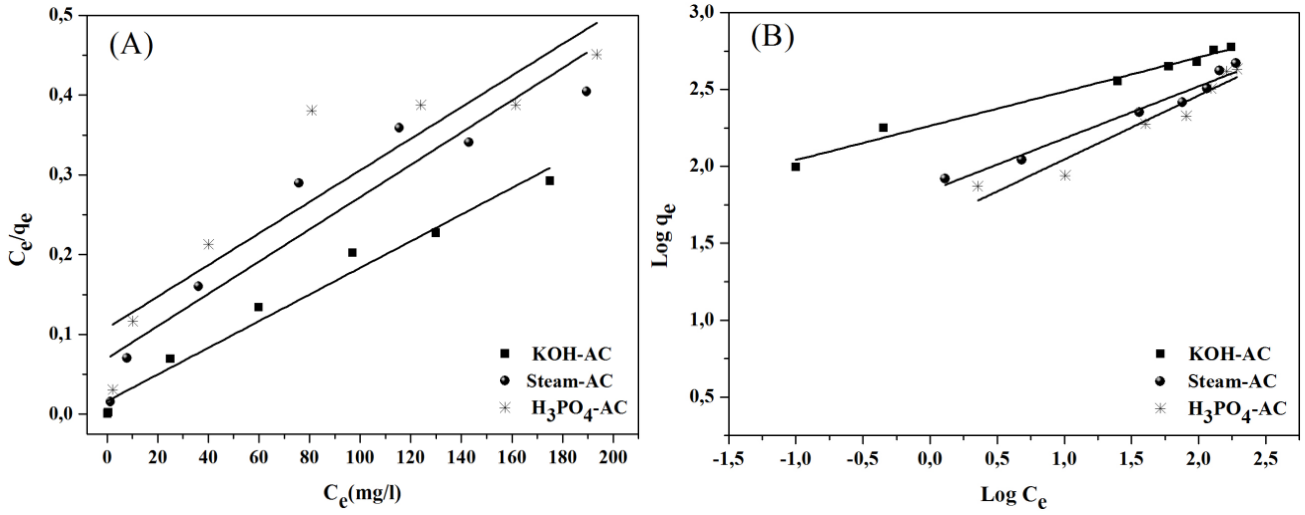

Figure 10: Langmuir (A) and Freundlich (B) isotherms for IC dye adsorption onto activated carbon samples.

The parameters of each model, calculated by regression from the linear form of the Langmuir and Freundlich isotherms (Figure 10), are represented in Table 4.

Table 4: Langmuir, Freundlich isotherm constants of IC adsorption on activated carbon

Materials	Langmuir			Freundlich		
	q_m(mg/g)	k_L (L/mg)	R^2	k_F (mg/g)(L/mg)$^{1/n}$	$1/n_F$	R^2
KOH-AC	598.80	0.10	0.97	183.53	0.22	0.98
H_3PO_4-AC	505.05	0.02	0.84	42.59	0.42	0.93
Steam-AC	495.05	0.03	0.89	69.60	0.34	0.97

Table 4 presented the isotherms constants, k_F and $1/n_F$ for Freundlich model, q_m and $k_L$for Langmuir model and linear R^2 for both models. The Freundlich isotherm was found to be linear over the entire concentration range studied with a good linear correlation coefficient (between 0.93 and 0.98), showing that data correctly fit the Freundlich relation. The values of Freundlich exponent $1/n_F$ were found less than 1, indicates the favorable adsorption [42]. For Langmuir isotherm, the values of R^2 (between 0.84 and 0.97) were much lower in comparison with the Freundlich model values, while the monolayer saturation capacity, q_{max}, was found relatively high compared to other adsorbent cited in the literature [2, 3, 9] supporting the hypothesis of monolayer coverage of dye onto sorbent. However, according to the R^2 value, the model of Freundlich appears to describe better the experimental data, than Langmuir isotherm. The adsorption process appears to occur randomly on a heterogeneous surface.

3.2.3. Thermodynamic study

Adsorption experiments were carried out at three different temperatures 293 K, 308 K and 323 K. For each temperature considered, the values of C_e and q_e corresponding to the equilibrium state were determined. Figure 11 shows the influence of temperature on adsorption capacities, it is found that the sorption of IC increases with an increase in temperature due to endothermicity of the sorption process. An increase in temperature produces an increase in the mobility of dye molecule and a possible increase in the porosity of the adsorbent [43, 44]. This may be due, also, to increasing in the number of active sites for the adsorption as the temperature increase [45]. Furthermore, a swelling effect in the internal structure of adsorbent may be produced with increasing temperature which allows more dye to penetrate further [46].

The change in standard free energy ($\Delta G°$) for adsorption process was calculated from the following equation:

$$\Delta G° = -RT\ln K_c \qquad (10)$$

Where K_c is the equilibrium constant expressed in $L.g^{-1}$, and can be calculated from Eq (11):

$$K_c = \frac{q_e}{C_e} \qquad (11)$$

The values of enthalpy change (ΔH°) and entropy change (ΔS°) can be determined, respectively, from the slope and intercept of plots of $\ln K_C$ versus 1/T (Eq.12):

$$\ln K_c = \frac{\Delta S^{\circ}}{R} - \frac{\Delta H^{\circ}}{RT} \qquad (12)$$

The changes in standard free energy (ΔG°), enthalpy (ΔH°) and entropy (ΔS°) of adsorption process were shown in Table 5.

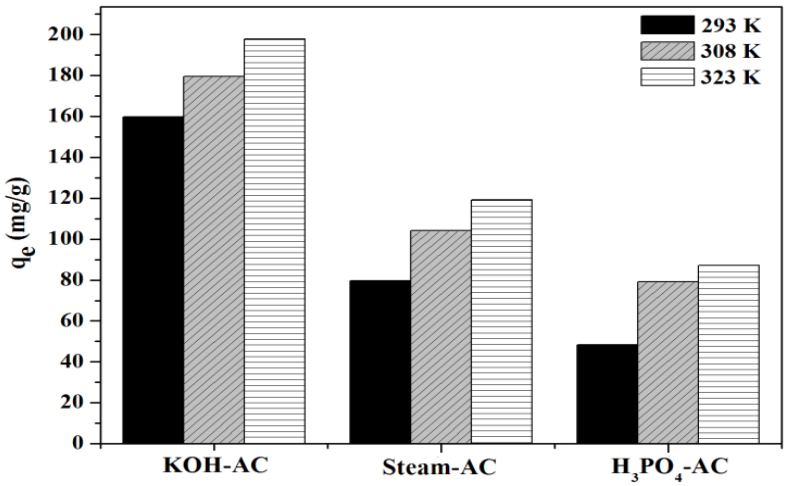

Figure 11: Effect of temperature on the sorption of IC onto activated carbon samples.

Table 5: Thermodynamic parameters of IC dye adsorption on prepared activated carbon.

Materials	Thermodynamic parameters				
	ΔG° (kJ mol^{-1})			ΔH°	ΔS°
	293 K	308 K	323 K	(kJ mol^{-1})	(J/K mol)
KOH-AC	-10.44	-12.16	-14.17	25.91	123.92
H_3PO_4-AC	-2.82	-4.81	-5.31	21.72	84.52
Steam-AC	-5.07	-6.10	-6.97	13.52	63.53

The negative value of the Gibbs free energy (ΔG°), obtained for dye adsorption on KOH-AC, Steam-AC and H_3PO_4-AC, indicates that the adsorption process has spontaneous nature. It was also observed from Table 5, that (ΔG°) becomes more negative as the temperature is increasing, revealing that the adsorption process is more favorable at high temperatures. The obtained values of ΔH° for all carbons was positive and lower than 84 kJ/mol, which confirm the endothermic nature of adsorption and the possibility of physical adsorption [47]. Table 5 shows also positive values of ΔS°, which indicate an increase of disorder and randomness at the solid solution interface of the adsorbent as a result of the adsorption. The comparison between the maximum uptake capacities (q_m) for IC of activated carbons prepared from olive wastes and other adsorbents reported in the literature are given in Table 6. The result shows that the maximum adsorption capacities obtained in this study are best or comparable to the results from the reported activated carbons.

Table 6: Comparison of adsorption capacities of indigo carmine onto some adsorbents.

Adsorbent	q (mg/g)	Reference
Commercial Activated Carbon (No. 1-I, Bamberg Co.)	135	Tamura et al. [48]
Microwave-treated activated carbon from peanut shell	159	Zhang et al. [49]
KOH activated carbon from pistachio shells 2.0 (KOH/char)	361	Wu et al. [50]
Steam activated carbon from pistachio shells 2.0 (KOH/char)	147	Wu et al. [50]
Carbon from fir wood by KOH etching and CO_2 gasification (FWKC1030)	359	Wu and Tseng [51]
NaOH-activated carbon from Fir wood (FWNa4)	912	Wu and Tseng [52]
Activated carbon doped with biogenic manganese oxides	460	Hu et al. [53]
KOH-AC from olive waste	599	This work
H_3PO_4-AC from olive waste	505	This work
Steam-AC from olive waste	495	This work

Conclusion

In this study the AC prepared from olive waste was used as an adsorbent to remove IC dye from aqueous solution. Three simplified kinetic models, pseudo-first order, pseudo-second-order, and intra-particle diffusion were tested to investigate the adsorption mechanism. The pseudo second-order kinetic model fits very well with the dynamical adsorption behavior of IC dye, the linear form of the Freundlich isotherm appears to produce a reasonable model than Langmuir isotherm, the values of Freundlich exponent $1/n_F$ were found less than 1, indicates the favorable adsorption. The values for the Gibbs free energy indicate that the adsorption of indigo carmine on prepared carbons is a spontaneous process. The positive values of ΔH° show the endothermic nature of adsorption.

From the results of this study we can draw as a conclusion that activated carbon prepared from olive-waste can be successfully used for the adsorption of indigo carmine dye from aqueous solutions exhibiting a good adsorption properties similar of higher than other adsorbents cited in the literature.

References

1. O'neill C., Hawkes F.R., Hawkes D.L., Lourenco N.D., Pinheiro H.M., Delee W., *J. Chem. Technol. Biotechnol.* 74 (1999) 1009.
2. Gutiérrez-Segura E., Solache-Ríos M., Colín-Cruz A., *J. Hazard. Mater.* 170 (2009) 1227.
3. Lakshmi U.R., Srivastava V.C., Mall I.D., Lataye D.H., *J. Environ. Manage.* 90 (2009) 710.
4. Flox C., Ammar S., Arias C., Brillas E., Viridiana Vargas-ZavalaA., Ridha A., *Appl. Catal. B: Environ*. 67 (2006) 93.
5. Secula M. S., Creţescu I., Petrescu S., *Desalination* 277 (2011) 227.
6. Gómez-Solís C., Juárez-Ramírez I., Moctezuma E., Torres-Martínez M., *J. Hazard. Mater*. 217–218 (2012) 194.
7. Agorku E.S., Kuvarega A.T., Mamba B.B., Pandey A.C., Mishra A.K., *J. Rare Earths* 33 (2015) 498
8. Ben Younes S., Sayadi S., *J. Molec. Cataly. B: Enzymatic* 87 (2013) 62.
9. De Oliveira Brito S.M., Carvalho Andrade H.M., Soares L.F., Pires de Azevedo R., *J. Hazard. Mat*er. 174 (2010) 84.
10. Prado A.G.S., Torres J.D., Faria E.A., Dias S.C.L., *J. Coll. Interf. Sci.* 277 (2004) 43.
11. Noorimotlagh Z., Darvishi Cheshmeh Soltani R., Khataee A.R., Shahriyar S., Nourmoradi H., *J. Taiwan Inst. Chem. Eng*. 45 (2014) 1783.
12. Stals M., Vandewijngaarden J., Wro´bel-Iwaniec I., Gryglewicz G., Carleer R., Schreurs S., *J Anal. Appl. Pyrol.* 101(2013) 199.
13. Ma X., Ouyang F., *Appl. Surf. Sci.* 268 (2013) 566.
14. Gao Y., Yue Q., Gao B., Sun Y., Wang W., Li Q., Wang Y., *J. Chem. Eng*. 217 (2013) 345.
15. Tan I.A.W., Ahmad A.L., Hameed B.H., *J. Hazard. Mater*. 154 (2008) 337–46.
16. Eddebbagh M., Abourriche A., Berrada M., Benzina M. and Bennamara A., *J. Mater. Environ. Sci*. 7 (6) (2016) 2021.
17. Bacaoui A., Yaacoubi A., Dahbi A., Bennouna C., Phan Tan Luu R.,Maldonado-Hodar F.J., Rivera-Utrilla J., Moreno-Castilla C., *Carbon* 39 (2001) 425.
18. Bacaoui A., Dahbi A. , Yaacoubi A., Bennouna C., Maldonado-Hódar F. J., Rivera-Utrilla J., Carrasco-Marian F., Moreno-Castilla C., *Environ. Sci. Technol*., 36 (2002) 3844.
19. Noszko L., Bota A., Simay A., Nagy L., *Period. Polytech. Chem. Eng*. 28 (1984) 293.
20. ASTM D4607– 94 (2006). ASTM International, 100 Barr Harbor Drive, United States.
21. Mittal A., Mittal J., Kurup L., *J. Hazard. Mater*. B137 (2006) 591.
22. Hashemian S., Sadeghi B., Mangeli M., *J. Ind. Eng. Chem*. 21 (2015) 423.
23. Sing K.S.W., Everett D.H., Haul R.A.W., et al., *J. Pure Appl. Chem*., 57 (1985) 603.
24. Stavropoulos G.G., Zabaniotou A.A., *Micropor. Mesopor. Mater*.82 (2005) 79.
25. Yardim M.F., Ekinci E., Minkova V., Razvigorova M., Budinova T., Petrov N., Goranova M., *Fuel* 82 (2003) 459.
26. Jagtoyen M., Derbishire F., *Carbon* 36 (7–8) (1998) 1085.
27. Salman J.M., Njoku V.O., Hameed B.H., *J. Chem. Eng*., 173(2) (2011) 361.
28. Budinova T., Ekinci E., Yardim F., Grimm A., Björnbom E., Minkova V., Goranova M., *Fuel Process. Technol.* 87 (2006) 899.

29. Wang Z., Nie E., Li J., Zhao Y., Luo X., Zheng Z., *J. Hazard. Mater*. 188 (2011) 29.
30. Marsh H., Rodriguez-Reinoso F.R., *Activated carbon.* 1st Edition, Elsevier Science, Amsterdam (2006).
31. Toles C.A., Marshall W.E., Johns M.M., *Carbon* 35 (1997).
32. Benadjemia M., Millière L., Reinert L., Benderdouche N., Duclaux L., *Fuel Process. Technol*. 92 (2011) 1203.
33. Lagergren S., *Handlingar* 24 (1898) 1.
34. Crini G., Peindy H.N., Gimbert F., Robert C., Sep. *Purif. Technol*. 53 (2007) 97.
35. Ho Y. S., Mckay G., *Trans. IChemE*. 76 (1998) 183.
36. Srivastava V.C., Swamy M.M., Mall I.D., Prasad B., Mishra I.M., *Colloids and Surf A: Physicochem. Eng. Aspects* 272 (2006) 89.
37. Weber J.R., Morris J.C., *J. Sanitary Eng. Division*: Am. Soc. Civil Eng. 89 (1963) 31.
38. Taran F., Nazemi A. H., Sadraddini A. A., Dinpazhuh Y., *J. Mater. Environ. Sci.* 7 (2016) 2082.
39. Langmuir I., *J. Am. Chem. Soc*. 40 (1918) 1361.
40. Moafi H. F., Ansari R., Ostovar F., *J. Mater. Environ. Sci*. 7 (2016) 2051.
41. Freundlich H.M.F., *J. Phys. Chem*. 57 (1906) 385.
42. Wang L., Zhang J., Zhao R., Li C., Li Y., Zhang C., *Desalination* 254 (2010) 68.
43. Khare S.K., Srivastava R.M., Panday K.K., Singh V.N., *Environ. Technol. Lett*. 9 (1988) 1163.
44. Dogan M., Alkan M., *Chemosphere* 50 (2003) 517.
45. Senthilkumaar S., Kalaamani P., Subburaam C.V., *J. Hazard. Mater*. 136 (2006) 800.
46. Singh K.P., Mohan D., Tondan G.S., Gosh D., *Ind. Eng. Chem. Res*. 42 (2003) 1965.
47. Ahmad R., Kumar R., *Appl. Surf. Sci*. 257 (2010) 1628.
48. Tamura T., Miyoshi T., Boki K., Tanada S., *Jpn. J. hyg*. 42 (1987) 858.
49. Zhang J., Zhou Q., Ou L. (2014), *Desalin. Water Treat*. DOI: 10.1080/19443994.2014.967729
50. Wu F.C., Tseng R.L., Hu C.C., *Microporous and Mesoporous Materials* 80 (2005) 95.
51. Wu F.C., Tseng R.L., *Journal of Colloid and Interface Science* 294 (2006) 21.
52. Wu F.C., Tseng R.L., *J. Hazard. Mater*. 152 (2008) 1256.
53. Hu Y., Chen X., Liu Z., Wang G., Liao S., *J. Environ. Manage*. 166 (2016) 512.

(2017) ; http://www.jmaterenvironsci.com